EXPERIMENTAL STUDY OF A VORTEX TUBE

Rafael Angelo Polisel
SISEA – Alternative Energy Systems Laboratory - Mechanical Eng. Dept. - Escola Politécnica da Universidade de São Paulo - Av. Prof Mello Moraes 2231, CEP 05508-900 - São Paulo, SP - Brasil
rafael.polisel@poli.usp.br

José R. Simões-Moreira
SISEA – Alternative Energy Systems Laboratory - Mechanical Eng. Dept. - Escola Politécnica da Universidade de São Paulo - Av. Prof Mello Moraes 2231, CEP 05508-900 - São Paulo, SP - Brasil
jrsimoes@usp.br

Abstract. *Vortex tube or Ranque-Hilsch tube is a quite simple moving parts free mechanical device which is basically formed by a cylindrical body having a compressed air inlet machined perpendicularly to it. As compressed air flows into the inlet it reaches the inner part of the tube tangentially describing a swirling path, which splits the incoming air into two flow streams to each one of the tube ends. In one of the ends the air is cooler than the intake air temperature, while in the other end the exiting air is warmer.*
The goal of this experimental study is to find out the best operational conditions by a parametric analysis. The variables studied are: different "hot" and "cold" cross sections; tube length; and intake compressed air pressure. In some cases, it was found a temperature difference of 36 ^{o}C between the "hot" and "cold" exits for a feeding air pressure of about 3.5 bar abs.
The tests have shown that the lengthier the tube, the higher the temperature difference. Increasing pressure also increases the temperature difference. An interesting find is that as the "hot" cross section was increased, there was a point where the device operated the best as seen from an analysis of the "cold" air exit. The paper reports several experimental results.

Keywords*: Ranque, Hilsch, Vortex, Air cooling.*

1. Introduction

The Vortex tube, also known as Ranque-Hilsch tube, was accidentally developed by the French physicist Gorges Ranque around the year 1930. Georges Ranque was carrying out experiments with a vortex generating device and noticed that cold air was released in the end of a tube while hot air left the tube in the other extremity. Ranque presented a paper to the Cientifique Society in 1933 describing his findings about the Vortex tube, but it raised questions about the authenticity of the phenomenon. His finding went without any notice until Rudolph Hilsch, a German physicist, showed a great interest for it exploring the subject more deeply, which drew attention to many people who erroneously believed he was the inventor of the vortex tube giving the name of "Hilsch Tube" to the device. (http://www.exair.com/vortextube/vt_theory.htm)

The Vortex tube is formed by a cylindrical tube in which compressed air is injected perpendicularly and tangentially to the internal tube wall trough a nozzle as schematically shown in Fig. 1. As the air reaches the inner part it describes a swirling path reaching up to 1.000.000 rpm as it advances in direction to the hot end exit, where only a fraction of it is released. The remaining air flow reflects back taking the central axial region and still rotating in the same direction to exit in the other end (cold exit). As illustrated in Fig. 1, swirling hot air leaves the tube in the peripherical cross sectional area at a higher temperature compared to the inlet air while swirling cold air leaves the tube in the central area of the other exit at a lower temperature.

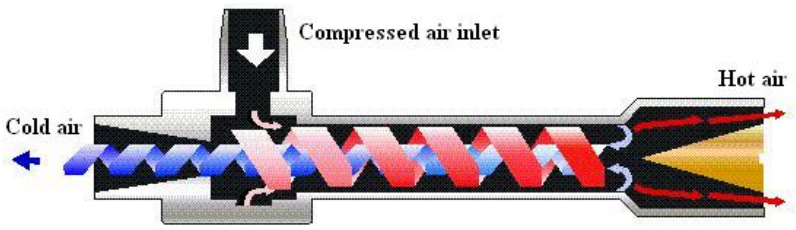

Figure 1. *Working principle of a Vortex tube. Compressed air is injected tangentially to the tube. The air stream is split into two other streams, one hot (right side) and the other cold (left side).*

2. Experimental Facility

2.1. Test Rig

Figure 2 shows a diagram of the test rig used to carry out the experiments. The Ranque-Hilsch tube is connected to a compressed air line and the injection pressure is set by a pressure controlling valve. Air injection pressure and temperature can be measured as indicated. A shut off valve blocks off the air if necessary.

Cold and hot air exits are connected to a PVC tube where instrumentation was fixed. A thermocouple was inserted in the flow. Exit velocities were taken using a digital anemometer.

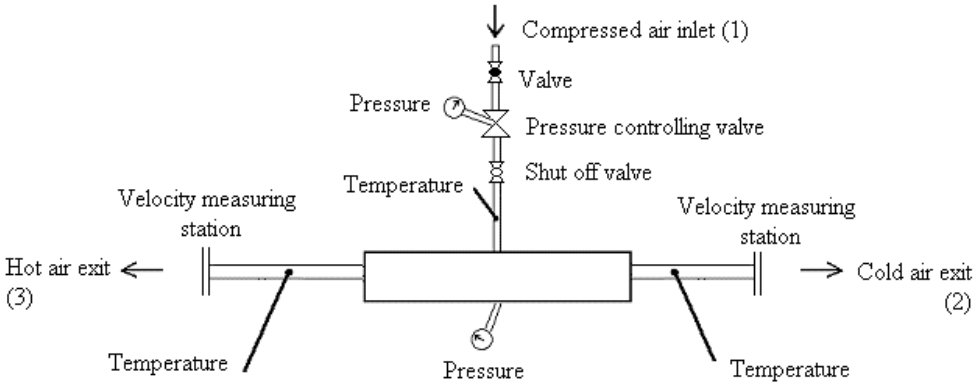

Figure 2. *Diagram of the test rig*

2.2. Prototype

Figure 3 presents a still picture of the Vortex tube assembled on the test rig base. Cold air exited on the left side and hot air on the right side. Inlet compressed air connection is also shown. Instrumentation taps can also be seen in that picture.

Figure 3. *Vortex tube prototype*

Figures 4 and 5 show details of some of the main parts of the Vortex tube. Fig. 4 shows details of the injection sleeve and the compressed air intake tap. Fig. 5 displays two still pictures of the inserts from which air flows out the device. Left insert is for cold air, while the other is for hot air. Notice that cold air flows out through the central part, where hot air leaves in the peripherical area of the tube.

Figure 4. C*ompressed air injection sleeve*

Figure 5. *Inserts from which cold air (left) and hot air (right) flows through before leaving the vortex tube*

3. Physical Modelling

3.1. Energy and Mass Balances

Considering the control volume enveloping the tube as illustrated in Fig. 6, a balance energy yields the following equation (Eq. 1):

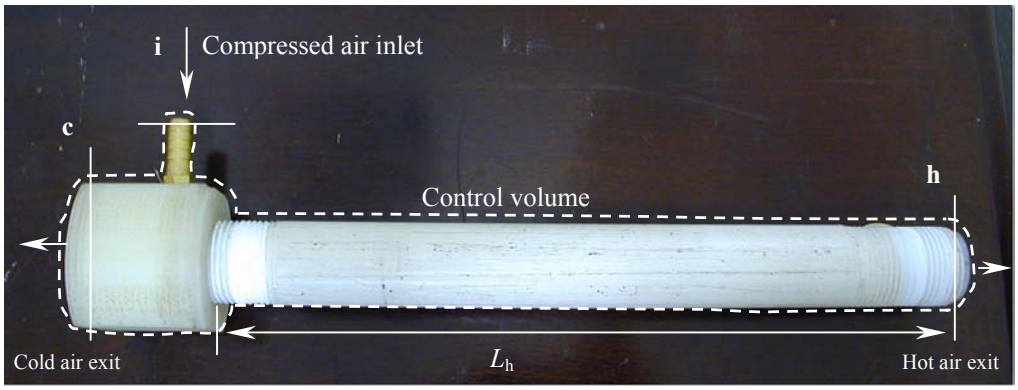

Figure 6. *Control volume enveloping the Ranque-Hilsch tube*

$$\frac{dE_{C.V.}}{dt} = \dot{Q}_{C.V.} - \dot{W}_{C.V.} + \sum \dot{m}_i (h_i + \tfrac{1}{2}V_i^2 + gZ_i) - \sum \dot{m}_o (h_o + \tfrac{1}{2}V_o^2 + gZ_o), \quad (1)$$

where, indexes "*i*" and "*o*" refer to inlet and outlet conditions, respectively. $E_{C.V.}$ is the instantaneous control volume total energy, $\dot{Q}_{C.V.}$ is the control volume heat exchange with the environment, $\dot{W}_{C.V.}$ is the shaft power, $\dot{m}$ is the mass flow rate, *h* is the specific enthalpy, *V* is the velocity in and out the control volume, *Z* is elevation, and *g* acceleration of gravity. The usual assumptions of steady state, adiabatic control volume, no shaft power and negligible kinetic and potential energy, the simple equation comes out.

$$\dot{m}_i.h_i = \dot{m}_h.h_h + \dot{m}_c.h_c, \quad (2)$$

since there are two exits, one "cold" and the other "hot", the outlets are indicated by the indexes "*c*" and "*h*", respectively. A further hypothesis may be assumed based on the ideal gas behavior. By assuming a constant specific heat at constant pressure, C_P, one may obtain the equation (Eq. 3),

$$\dot{m}_i.T_i = \dot{m}_h.T_h + \dot{m}_c.T_c. \quad (3)$$

Let μ be defined as the mass flow ratio between "cold" and inlet mass flow rates, i. e., ($\mu = \dot{m}_c / \dot{m}_i$), which is called "cold mass ratio". That magnitude in combination with the mass conservation equation, $\dot{m}_i = \dot{m}_h + \dot{m}_c$, Eq. (3) yield the following equation (Eq. 4),

$$T_i = (1-\mu).T_h + \mu.T_c, \quad (4)$$

which implies that

$$\mu = \frac{T_i - T_h}{T_c - T_i}. \quad (5)$$

The set of equations above where used to compare experimental results.

3.2. Experimental Data Reduction

Values of cold mass ratio, μ, were obtained experimentally from exit velocity measurements as shown below. Eq. (6) is obtained directly from μ definition,

$$\mu_{meas} = \frac{\dot{m}_c}{\dot{m}_i} = \frac{\dot{m}_c}{\dot{m}_c + \dot{m}_h} = \frac{1}{1 + \frac{\dot{m}_h}{\dot{m}_c}}, \tag{6}$$

where, $\dot{m}_c = \rho_c \cdot A_c \cdot V_c$ and $\dot{m}_h = \rho_h \cdot A_h \cdot V_h$ are the mass flow rates. By substituting these equations into Eq. (6), also considering that $A_c = A_h$ for the tested setup, then one can obtain the (indirectly) measured cold mass ratio, μ_{meas}, which is given by

$$\mu_{meas} = \frac{1}{1 + \frac{\dot{m}_h}{\dot{m}_c}} = \frac{1}{1 + \frac{\rho_h \cdot A_h \cdot V_h}{\rho_c \cdot A_c \cdot V_c}} = \frac{1}{1 + \frac{\rho_h \cdot V_h}{\rho_c \cdot V_c}}. \tag{7}$$

Since both "cold" and "hot" exits are discharging into local environment, it is possible to show that the density ρ is the reciprocal of the absolute temperature, i. e.,

$$\rho = \frac{P}{R \cdot T} \Rightarrow \rho \approx \frac{1}{T}. \tag{8}$$

Finally, by substituting this last equation into Eq. (7), it results in

$$\mu_{meas} = \frac{1}{1 + \frac{T_c \cdot V_h}{T_h \cdot V_c}}. \tag{9}$$

4. Parametric Analysis

A parametric study was carried out in order to find out the best operational conditions of the Ranque-Hilsch tube. The study had its starting point based on the works of Staschower and Rotter (2003) and Piralishvili (1994). These previous work identified that three geometrical parameters dominate tube operation. The first two important parameters are the exit cold and hot areas, which comprise the first two columns in Table 1. The third governing geometrical parameter is the "hot" side tube length. Table 1 shows the magnitude values used in this work. As far as feeding pressure concerns, it has been found (Staschower and Rotter, 2003) that the higher the pressure, the higher the temperature difference between "hot" and "cold" exits. The present experiments were carried out at the highest possible pressure the compressor would supply at the mass flow rate being tested (0.35 MPa).

A experiment matrix was setup by combining all possibilities of the geometrical parameters, i. e., 4×5×5, giving a total of 100 experiments.

Table 1. *Geometrical magnitudes tested*

Cold area (mm^2)	Hot area (mm^2)	Hot tube length (mm)
19.6	31.4	300
28.3	42.4	400
38.5	56.5	500
63.6	75.4	600
-	100.5	700

5. Experimental Results and Analysis

Figures 7 to 11 show the main experimental results for all the possible combinations. In all cases the graphics has ΔT_c as function of hot area (A_h), where ΔT_c is the difference between the inlet temperature and the cold exit temperature. Fig. 7 is for hot tube length (L_h) of 300 mm, Fig. 8 for L_h = 400 mm, Fig. 9 for L_h = 500 mm, Fig. 10 for L_h = 600 mm, and Fig. 11 for L_h = 700 mm. As seen in figures sequence, for each hot tube length four test sequences were carried out having the cold area exit values indicated in Table 1. Exit temperatures were also measured, but only the cold ones are shown for sake of saving space. For all tests, it has been shown that the highest temperature difference, i.e., the smallest cold temperature, systematically occurred for the larger area exit tested (A_c = 63.6 mm^2).

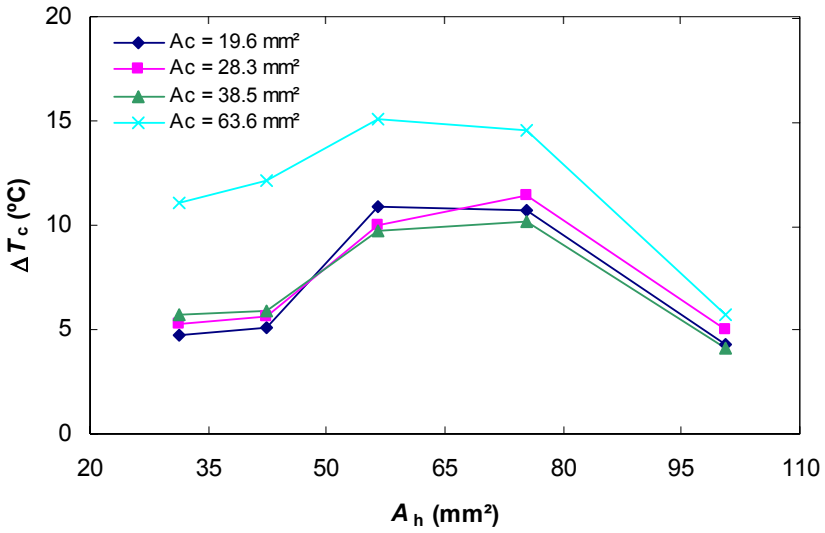

Figure 7. *Temperature drop for L_h = 300 mm*

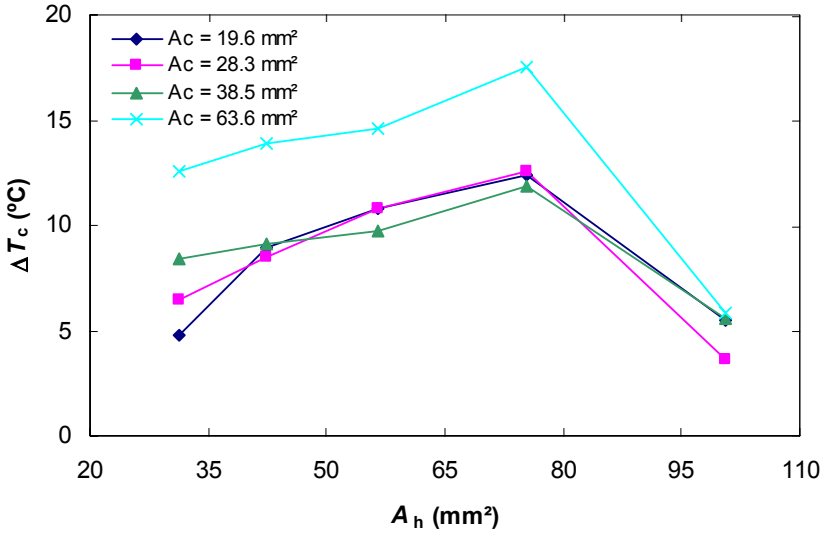

Figure 8. *Temperature drop for L_h = 400 mm*

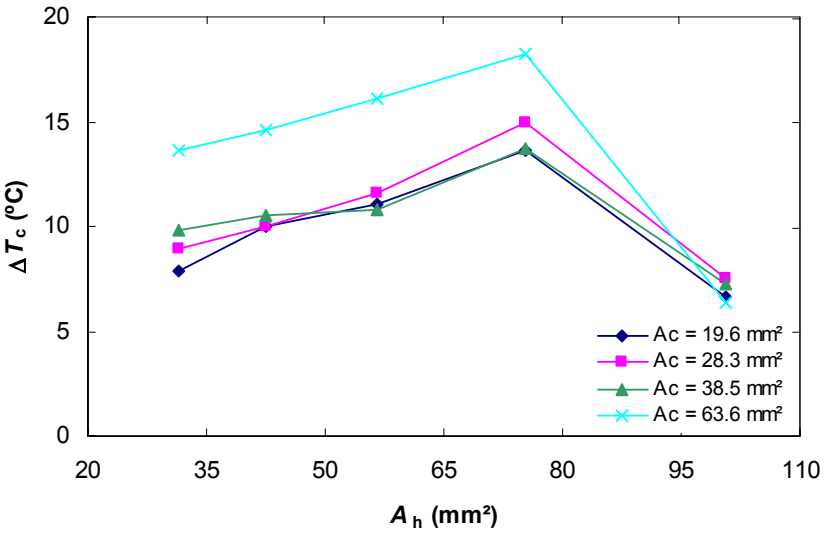

Figure 9. *Temperature drop for L_h = 500 mm*

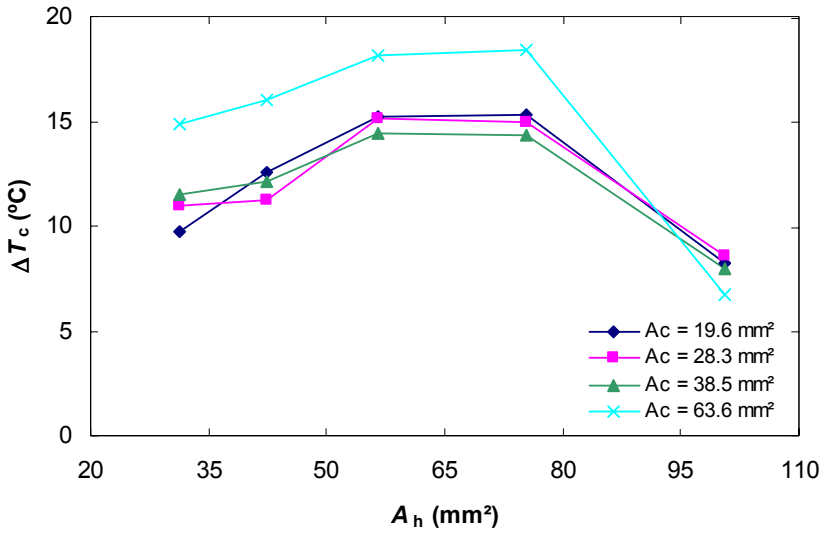

Figure 10. *Temperature drop for L_h = 600 mm*

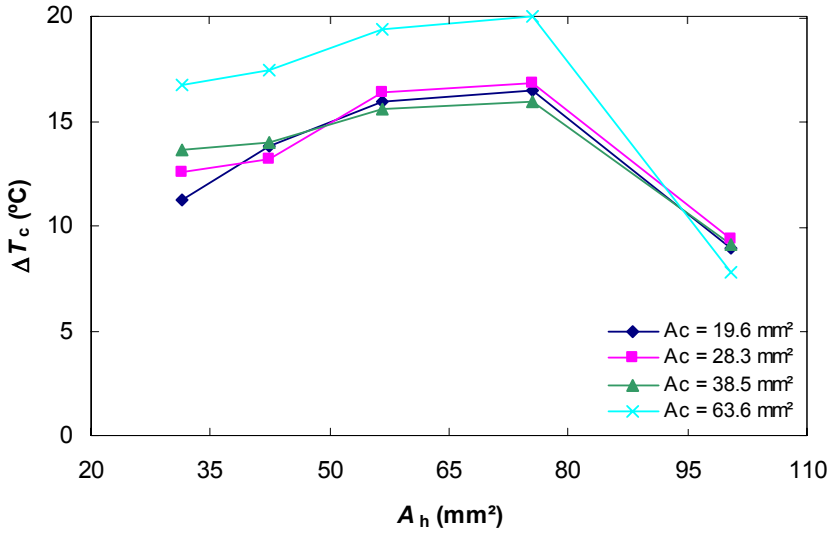

Figure 11. *Temperature drop for L_h = 700 mm*

Another important conclusion one can draw refers to the influence of the hot area (A_h). As a general rule, as the hot area is increased, the temperature difference increases as well up to a point of maximum, to decrease afterwards. From an analysis of Figs. 7 to 11, the maximum ΔT_c occurred between the hot areas A_h = 56.5 mm^2 and 75.4 mm^2, for all the conducted tests. Finally, the last important observation regarding optimal operation conditions can be drawn observing the graphics in Fig. 12. This graphics was devised from experiments with the best cold area, i. e., A_c = 63.9 mm^2 for all studied cases. As one can see in that figure, the lengthier the hot tube portion, L_h, the better the tube operate. A maximum temperature drop ΔT_c of 20 ^{o}C was achieved with the device designed in here.

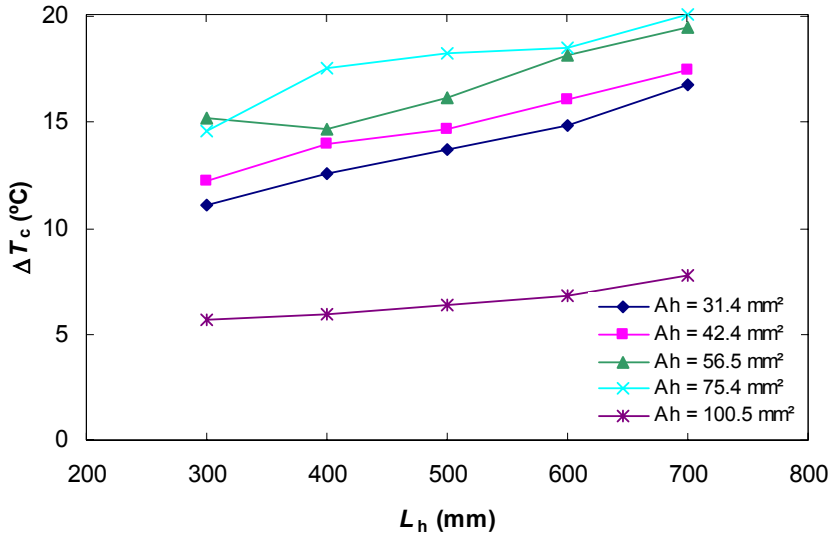

Figure 12. *Hot tube length influence for A_c = 63.6 mm²*

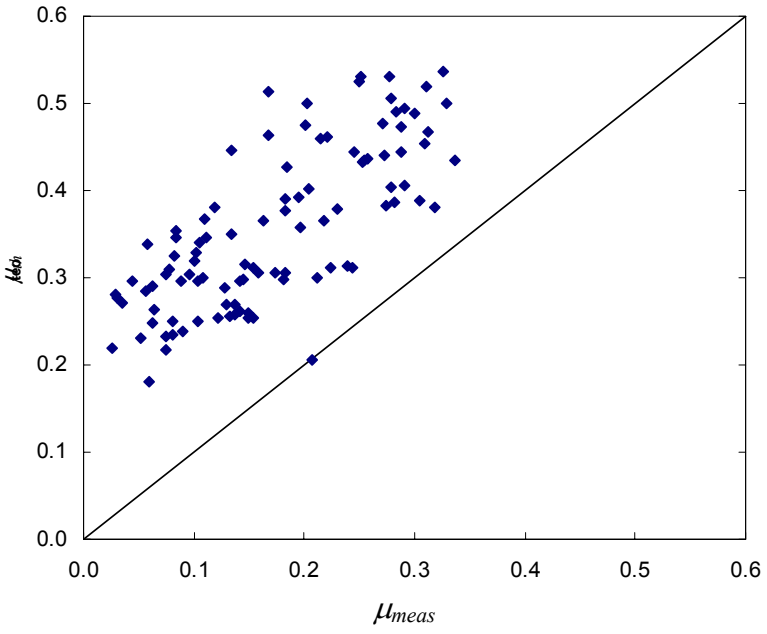

Figure 13. *First Law of Thermodynamics – Comparison of μ_{th} x μ_{meas}*

A last analysis was carried out regarding closing the First Law of Thermodynamics. The graphics in Fig. 13 indicated the measured cold mass ratio, μ_{meas}, versus the theoretical value, μ_{th}. Measured value was inferred from velocity and temperature measurements of cold and hot exits and data reduction according to Eq. (9). Theoretical cold mass ratio, μ_{th}, was calculated from Eq. (5), which is derived from the First Law. A perfect correlation would furnish all the experimental data lining up over the 45° line in the graphics in Fig. 13. However, for authors' surprise the graphics clearly shows that the measured value systematically felt always below the theoretical one. This finding made the authors to question the velocity measuring equipment. It is now under investigation to find out the reason why such a discrepancy.

6. Conclusions

The present parametric study of a Ranque-Hilsch or Vortex tube set the limits of some important operational performance and established a geometrical influence over the overall behavior. As a first conclusion, it was found that a larger exiting cold air area increases the temperature drop, i.e., the difference between the inlet and cold air exit temperatures at least for the device and the area range studied here. Another important conclusion is that the lengthier the hot portion of the tube the colder is the air. On the other hand, an interesting finding was related to the hot air exit area. For the area range tested here, there was a hot area range for which the temperature drop reached a point of maximum. The best operating conditions were: hot tube length equals to 700 mm, cold air exit area equals to 63.6 mm^2, and hot air exit area within the range of 56.5 to 75.4 mm^2. Of course these values must be refined in future through a test mapping procedure to thoroughly cover all the range of interest with experimental data. However, it is good to recall that this is a real time consuming task. New checks will be done with the velocity measuring system which showed to be inadequate for the present tests.

Finally, as a last comment, the influence of the feeding pressure was not properly analyzed due to the limitations of the air compressor that could not deliver enough mass flow rate at certain pressure levels.

7. Acknowledgments

The authors would like to acknowledge FAPESP and CNPq (Brazil) for personal support, respectively.

8. References

ATRX - THE AIR RESEARCH TECHNOLOGY COMPANY (www.artxltd.com/vortex/principle.shtml). First access: Dec/2003.

ATRX - THE AIR RESEARCH TECHNOLOGY COMPANY (www.artxltd.com/vortex/apps.shtml). First access: Dec/2003.

EXAIR (www.exair.com/vortextube/vt_theory.htm). First access: Nov/2003.

Lewis, J. and Bejan, A., 1999, "Vortex tube optimization theory", *International Journal of Heat and Mass Transfer*, pp. 931-943.

Piralishvili, Sh. A. and Polayev, V. M., 1996, "Flow and thermodynamics characteristics of energy separation in a double-circuit vortex tube – An experimental investigation", *Experimental Thermal and Fluid Science*, Elsevier Science.

Staschower, M. and Rotter, B., 2003, "Estudo de um Tubo de Ranque-Hilsch", Mechl Eng. Dept. at Escola Politécnica da Universidade de São Paulo – Final Graduation Project, São Paulo, Brasil.

Wylen, G. J. V., Sonntag, R. E. and Borgnakke, G., 2003, *Fundamentals of Classical Thermodynamics*, John Wiley & Sons, 6ª ed., New York.